Supporting Information

Cyanobenzene-modified polymer acceptors for high-efficiency all-polymer solar cells with low energy loss

Xinya Ran,[a,b] Dingding Qiu,[a] Jianqi Zhang,[a] Jing Li,[c] Zhixiang Wei,*[a,b] Kun Lu*[a,b]

1. *[a] CAS Key Laboratory of Nanosystem and Hierarchical Fabrication, National Center for Nanoscience and Technology, Beijing 100190, China*
2. *[b] Sino-Danish Center for Education and Research, Sino-Danish College, University of Chinese Academy of Sciences, Beijing 100049, China*
3. *[c] Key Laboratory of Photochemical Conversion and Optoelectronic Materials, Technical Institute of Physics and Chemistry, Chinese Academy of Sciences, Beijing 100190, China*

1 Experimental Section

1.1 Synthesis

All reactions were set up using standard Schlenk techniques and carried out under a N_2 atmosphere with dry solvents. Commercially available chemicals were obtained from Hyper Chemical Company, Bide Pharmatech Ltd, Alfa Aesar, J&K, Sigma-Aldrich, and TCI and used as received unless otherwise stated. Analytical thin layer chromatography (TLC) was performed on silica gel 60 F254 glass plates. TLC plates were visualized by exposure to short wave ultraviolet light (254 nm, 365 nm) and/or iodine. All the solvents used in the experiment are of analytical purity and are used directly without purification.

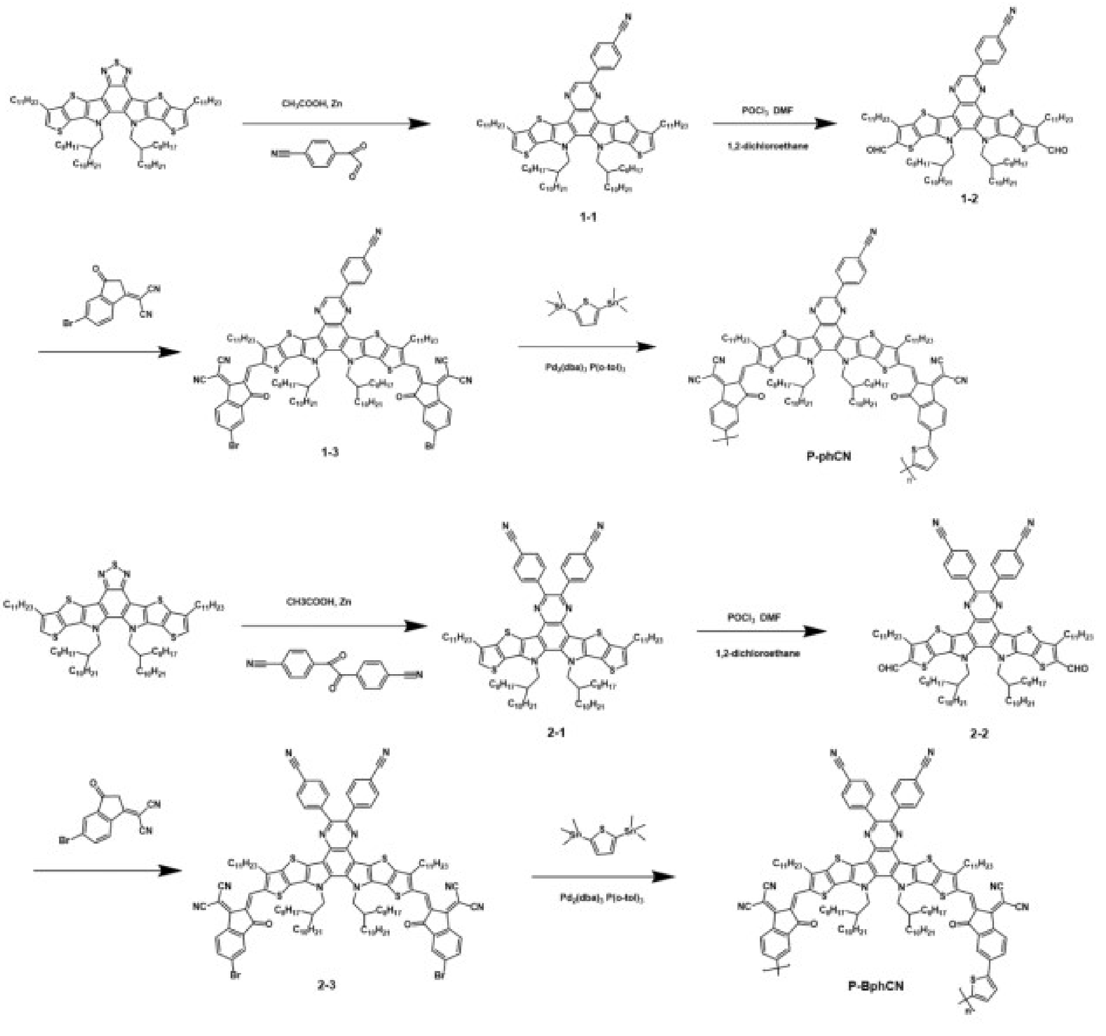

Scheme S1. The synthetic routes for the monomers and polymer acceptors.

Compound 1-1. To a solution of compound 1(500 mg, 0.47 mmol) in acetic acid (50 mL) was added zinc powder (1213 mg, 18.67 mmol) in one portion. Then the mixture solution was heated to 90°C for 5 h. After the solution was cooled at room temperature, the solid was removed by filtration. Transfer the filtrate to a three-tip flask containing 4-(2-oxoacetyl) benzonitrile (214.8 mg, 1.35 mmol), then the mixture solution was heated to 110°C for 20 h. After cooling to room temperature, washed with saturated salt water and methylene chloride. The solvent was removed under reduced pressure. The crude product was subsequently purified by column chromatography on silica gel to afford compound 1-1 as yellow oily solid (200 mg, 40% yield). ^{1}H NMR (400 MHz, $CDCl_3$) δ 9.51 (s, 1H), 8.59 (d, *J* = 8.4 Hz, 2H), 7.96 (d, *J* = 8.4 Hz, 2H), 7.06 (t, *J* = 11.5 Hz, 2H), 4.69 (d, *J* = 7.8 Hz, 4H), 3.80 – 2.64 (m, 4H), 2.24 (s, 2H), 1.89 (m, 4H)1.55 – 0.58 (m, 82H).

Compound 1-2: Compound 1-1 (200 mg, 0.17 mmol) was dissolved into chloroform (20 mL) in a three-neck flask. The solution was flushed with nitrogen at 0°C for 30 min. Then the fresh Vilsmeier-Haack reagent (0.3 mL $POCl_3$ and 0.9 mL DMF) was added dropwise to the solution at 0°C. After stirring at 0 °C for 30 min, the solution was warmed to 65°C and reacted for 4 h under nitrogen protection. The mixture was cooled to room temperature, the reaction was quenched with saturated $NaHCO_3$ solution and allowed to stir at room temperature for 1 h. The organic layer was separated, and the aqueous phase was extracted with CH_2Cl_2 for three times. The combined organic layer was washed with brine, dried over Na_2SO_4, filtered, and concentrated under reduced pressure. The crude product was purified with column chromatograph on silica gel to give compound 1-2 as an orange solid. (200 mg, 90% yield). ^{1}H NMR (400 MHz, $CDCl_3$) δ 10.08(d, J = 4.2 Hz, 2H), 9.33 (s, 1H), 8.20 (m, 2H), 7.21-7.18 (m, 2H), 4.62 (d, J = 7.8 Hz, 4H), 3.28 (m, 4H), 2.20 (s, 2H), 1.89 (m, 4H), 1.53 – 0.60 (m, 82H).

Compound 1-3: INCN-Br (271 mg, 1 mmol) and compound 1-2 (200 mg, 0.1 mmol) were added to a solvent mixture of chloroform (20 mL). After 0.8mL pyridine were added, the mixture was stirred at 65°C overnight. After cooling to room temperature, the reaction mixture was poured into water and extracted several times with chloroform. Removed solvent by reduced pressure and the residue was purified on a silica-gel column chromatography using chloroform as eluent to give compound 1-3 as black solid (200 mg, 90% yield). ^1H NMR (400 MHz, $CDCl_3$) δ 9.49 (s, 1H), 9.21 (d, *J* = 5.2 Hz, 2H), 8.56 (dd, *J* = 18.4, 8.4 Hz, 4H), 8.07 (d, *J* = 1.8 Hz, 2H), 7.99 (d, *J* = 8.4 Hz, 2H), 7.88 (dt, *J* = 8.5, 1.8 Hz, 2H), 4.87 (d, *J* = 4.4 Hz, 4H), 3.29 (dt, *J* = 15.6, 7.8 Hz, 4H), 2.24 (s, 2H), 2.04 – 1.81 (m, 4H), 1.65 – 0.72 (m, 114H).

Compound 2-1: Compound 2-1 was synthesized by similar procedure as compound 1-1 with compound 1 and compound 4,4'-oxalyldibenzonitrile. The final product was obtained as orange solid (200 mg, 90% yield). ^1H NMR (400 MHz, $CDCl_3$) δ 7.90 (t, J = 15.5 Hz, 4H), 7.78 (d, J = 8.4 Hz, 4H), 7.05 (d, J = 19.5 Hz, 2H), 4.70 (d, J = 7.8 Hz, 4H), 2.88 (t, J = 7.6 Hz, 4H), 2.17 (d, J = 5.6 Hz, 2H), 1.89 (m, 4H), 1.50 – 0.55 (m, 82H).

Compound 2-2: Compound 2-2 was synthesized by similar procedure as compound 1-2. The final product was obtained as orange solid (180 mg, 90% yield). ^1H NMR (400 MHz, $CDCl_3$) δ 10.19 (s, 2H), 7.81 (d, J = 8.0, 5.5 Hz, 4H), 7.24 (t, J = 8.7 Hz, 4H), 4.82 (d, J = 7.2 Hz, 4H), 3.26 (m, 4H), 2.18 (s, 2H), 2.01 – 1.91 (m, 4H), 1.52 – 0.50 (m, 82H).

Compound 2-3: Compound 2-3 was synthesized by similar procedure as 1-3 between compound 2-2 and INCN-Br. The final product was obtained as black solid (180 mg, 90% yield). ^1H NMR (400 MHz, $CDCl_3$) δ 9.21 (s, 2H), 8.60 (d, J = 8.4 Hz, 2H), 8.07 (d, J = 1.8 Hz, 2H), 7.89 (dd, J = 12.3, 5.1 Hz, 6H), 7.82 (d, J = 8.3 Hz, 4H), 4.87 (d, J = 7.7 Hz, 4H), 3.28 (t, J = 7.7 Hz, 4H), 2.23 (d, J = 5.4 Hz, 2H), 2.00 – 1.81 (m, 4H), 1.68 – 0.53 (m, 114H).

P-phCN: Under nitrogen protection, compound 1-3 (100 mg, 0.047 mmol), 2,5-bis(trimethylstannyl)thiophene (12.2 mg, 0.05 mmol), $Pd_2(dba)_3$ (0.8 mg) and $P(o\text{-}Tol)_3$ (1.1 mg) and degassed toluene (2 mL) were added to a 10 mL reaction tube. After the reaction mixture was stirred at 110 °C for 5 h. Then the mixture was poured into methanol (20 mL) and precipitation occurred. Then the resulting mixture was filtered. The obtained crude polymer was dissolved in warm chloroform and purified through a silica gel column with chloroform (100~200 mesh). The collected chloroform solution was concentrated and precipitated in methanol to get P-phCN as a dark solid (95 mg, 85% yield)

P-BphCN: The synthesis of P-BphCN was exactly the same as that of P-phCN, except that raw material compound 2-3 was replaced by compound 1-3. (90 mg, 81% yield).

2. Measurements and instruments

^{1}H NMR was obtained on a Bruker Avance III 400 NMR Spectrometer (operating at 400 MHz, using $CDCl_3$ as solvent using tetramethylsilane as internal standard).

The UV-vis absorption was measured by Shimadzu UV-3600 spectrophotometer. All solutions were diluted to 1×10^{-5} M.

Electrochemical cyclic voltammetry (CV) was conducted in an electrochemical workstation (VMP3 Biologic, France) with a Pt disk coated with blend film, a Pt plate, and an Ag^+ /Ag electrode acting as the working, counter, and reference electrodes, respectively, in a 0.1 mol/L tetrabutylammonium phosphorus hexafluoride (Bu_4NPF_6) acetonitrile solution. The experiments were calibrated with the standard ferrocene/ferrocenium (Fe) redox system and the assumption that the energy level of Fe is 4.8 eV below vacuum.

Theoretical calculations: The molecular geometries were optimized by the Gaussian program with a functional of B3LYP and a basis set of 6-31G(*d*, *p*). The long alkyl chains were replaced by methyl or isopropyl groups for saving computation time.

Devices fabrication: The conventional devices were fabricated with a structure of ITO/PEDOT:PSS (or 2PACz)/active layer/PNDIT-F3N/Ag. The ITO-coated glasses were cleaned under sonication for 30 minutes with detergent, deionized water, ethanol, and isopropyl alcohol sequentially. After drying, the substrates were treated with UV-ozone for 15 minutes. For PEDOT:PSS-based devices, PEDOT:PSS was deposited by spin-coating under 4000 rpm for 30 s onto ITO substrate and then thermally annealed for 15 minutes at 150 °C. Then acceptor materials were dissolved in chloroform (CF) solvent and then stirred at 50 °C for 60 minutes. 1-Chloronaphthalene (CN) was then added into the solvent. The blend solution was spin-coated at 3000 rpm for 30 seconds to form a thin film on the substrate. After thermal annealing at 100 °C for 10 min, PNDIT-F3N (0.5 mg mL^{-1}, in methanol with 0.5% v/v acetic acid) was spin-coated onto the top of the active layer as an electron transport layer at 3000 rpm for 30 s. Finally, a layer of Ag with a thickness of 150 nm was vacuum-deposited under 5×10^{-5} Pa. Except for the fabrication of PEDOT:PSS layer, the other processes were all carried out in a nitrogen-filled glovebox.

The current density–voltage (*J–V*) characteristics were collected using a Keithley 2400 Source under an AM 1.5G spectrum from a solar simulator.

The external quantum efficiency (EQE) measurements of the devices were performed in the air with an Oriel Newport system (Model 66902).

Transient photocurrent (TPC) and transient photovoltage (TPV) were measured by applying a 488 nm solid-state laser (Coherent OBIS CORE 488LS) with a pulse width of ~30 ns. The current traces were recorded by a mixed domain oscilloscope (Tektronix MDO3032) by converting the registered voltage drop across a 2 Ω resistor load connected in series to the solar cell. The photovoltage traces were registered by the oscilloscope with an external 10 MΩ resistor in series.

Space-Charge Limited Current (SCLC) Measurement

Hole and electron mobilities were measured by the space-charge limited current (SCLC) method with hole-only devices and electron-only devices. The hole-only devices adopted ITO/PEDOT:PSS/active layer/MoO_x/Ag structure, while electron-only devices adopted ITO/ZnO/active layer/PNDIT-F3N/Ag structure. An SCLC model was used mathematically expressed as:

$$J=\frac{9}{8}\varepsilon_0\varepsilon_r\mu_0\frac{(V-V_{bi})^2}{L^3}\exp\left(0.89\gamma\sqrt{\frac{V-V_{bi}}{L}}\right)$$

Where ε_0, ε_r is the dielectric constant of the semiconductor layer, μ_0 is the zero-field mobility, V_{bi} is the built-in potential due to the anode-cathode work function offset, L is the thickness of the active layer, and γ is the field-dependence coefficient.

Transient absorption (TA) spectroscopy was conducted using the Helios (Ultrafast) pump probe System in collaboration with a Regenerative Amplified Laser System (Coherent). An 760 nm pulse with a repetition rate of 1 kHz, a length of 100 fs, and an energy of 7 mJ per pluse, was generated by a Ti: sapphire amplifier (Astrella, Coherent). Then the 800 nm pulse was then divided into two parts using a beam splitter. One part was directed into an optical parametric amplifier (TOPAS, Coherent) to generate the pump pulses at various wavelength. The other part was focused onto sapphire and YAG plates to generate white light supercontinuum as the probe beams with spectra ranging from 420-800 nm and 750-1600 nm, respectively. The time delay between pump and probe was controlled by a motorized optical delay line with a maximum delay time of 8 ns. The pump pulse is chopped by a mechanical chopper with 500 Hz and then focused on to the mounted sample with probe beams. The probe beam was collimated and focused into a fiber-coupled multichannel spectrometer with CCD sensor. The energy of pump pulse was measured and calibrated by a power meter (PM400, Thorlabs). All the samples were prepared on the quartz substrate. The pump wavelength was set to 760 nm to selectively excite the acceptor in SD films.

Fourier-transform photocurrent spectroscopy external quantum efficiency (FTPS-EQE) measurements were carried out by an integrated system (PECT600, Enlitech).

Electroluminescence external quantum efficiency ($\mathrm{EQE_{EL}}$) was obtained by applying an external voltage/current source through the integrated device (REPS, Enlitech). $\mathrm{EQE_{EL}}$ measurements were performed for all devices according to the optimal device preparation conditions.

The E_{loss} in organic solar cells can be divided into three parts as follows:

$$E_{loss}=E_g^{pv}-qV_{OC}$$

$$=\left(E_g^{pv}-qV_{OC}^{SQ}\right)+\left(qV_{OC}^{SQ}-qV_{OC}^{rad}\right)+\left(qV_{OC}^{rad}-qV_{OC}\right)$$

$$=\left(E_g^{pv}-qV_{OC}^{SQ}\right)+qV_{OC}^{rad,\ below\ gap}+qV_{OC}^{non\text{-}rad}$$

$$=q\Delta V_1+q\Delta V_2+q\Delta V_3$$

$$=\Delta E_1+\Delta E_2+\Delta E_3$$

In this formula, q is the elementary charge; V_{OC}^{SQ} is the maximum voltage in the Shockley–Queisser (SQ) limit model, and V_{OC}^{rad} is the open-circuit voltage with only radiative recombination in the device.

Urbach energy calculation: Since the s-EQE method is suitable for highly sensitive absorption measurements and the EQE is direct proportion to the absorbance according to: The values of E_u could be obtained from the s-EQE curves by an exponential fit.

$$EQE(E)\propto a(E)\propto e^{\frac{E-E_g}{E_u}}$$

$$EQE=Ae^{\frac{E-E_g}{E_u}}$$

$$lnEQE=\frac{1}{E_u}E+B$$

The measurement of in-situ UV-vis: a specially designed spin coater, which allows a detective beam to pass through the center of the fabricating devices, was applied to measure the in-situ UV-vis spectrum. An F-20 spectrometer from filmetrics was used to record the spectrum, and the time revolution of the spectrum was 5 ms. Firstly, the ITO glass substrate with PEDOT:PSS is placed onto the spin coater, the probe beam from the spectrometer passes through the substrate to the detector at the bottom of the spin coating machine. Absorption baseline was taken with substrate before each coating session. Secondly, the same spin coat procedure for device fabrication is conducted, while the spectrometer records the absorption spectrum changes over time. The sampling interval of the spectrometer is set to 4 ms. Finally, stop recording data after detecting no spectral changes, and the test ends.

Contact angles were measured on the neat donor and acceptor films with the contact angle meter (Theta Flex, Biolin) by using two different solvents (water and glycerol). The Flory-Huggins interaction parameter can be written as the formula below:

$$\chi_{ij}=K\left(\sqrt{\gamma_i}-\sqrt{\gamma_j}\right)^2$$

Where K is a positive constant, where γ_i and γ_j are the surface energy of the donor and acceptor materials, respectively.

Atomic force microscopy (AFM) was performed by Bruker Multimode 8 in Scan Asyst Mode in air, operating platform in tapping mode. The samples were made by spinning coating the active layers on the PEDOT:PSS layer.

Transmission electron microscopy (TEM) images were acquired on Tecnai G2 F20 U-TWIN TEM instrument. The samples were made by using water to dissolve the PEDOT:PSS layer and getting the floating active layer to the TEM grids.

Grazing incidence wide-angle X-ray scattering (GIWAXS) characterizations were conducted at XEUSS SAXS/WAXS equipment.

Time-resolved PL Experiments: The in-situ PL spectra were measured using a spectrometer. The light source was a halogen lamp. The spin-coating process is controlled as the same for the device fabrication. The instrument model is ATP2002H, with an excitation wavelength of 550 nm, an acquisition wavelength range of 200 nm–1000 nm, a microsecond-level resolution, a data acquisition interval of 40 μs, and an integration time of 10 ms. No electrical bias was applied during the test, and the test environment had a relative humidity of 11.7% and a temperature of 20.7 °C.

2 Supplementary Figures

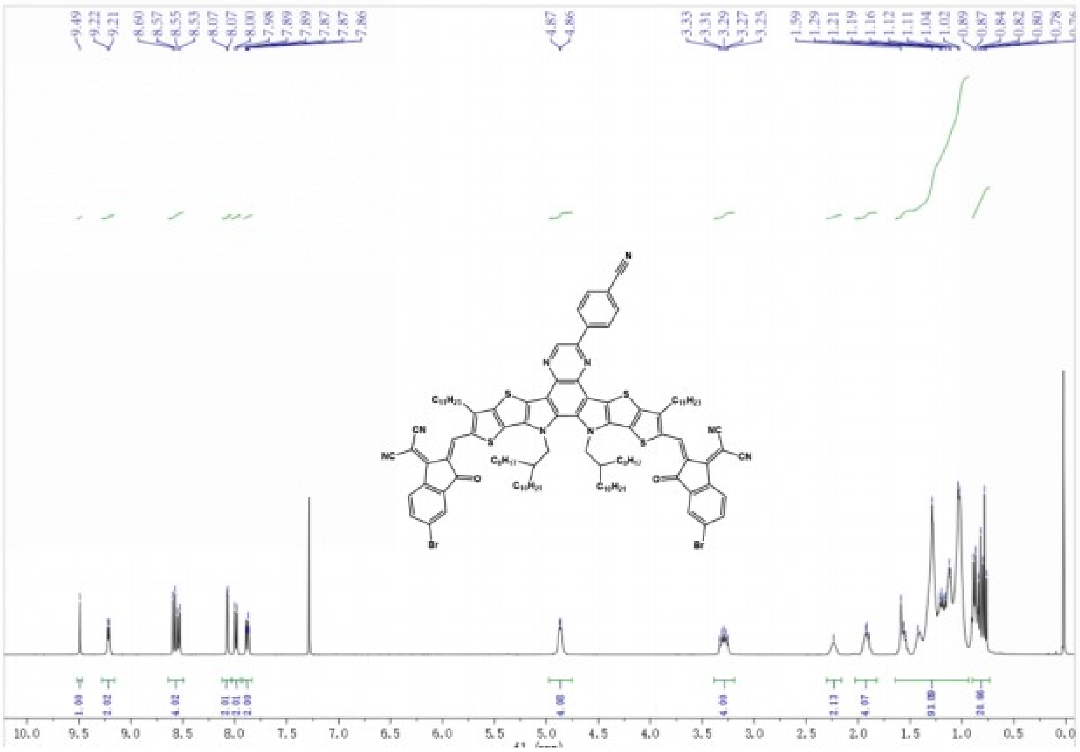

Fig. S1 ^{1}H NMR spectrum of P-phCN monomer in $CDCl_3$.

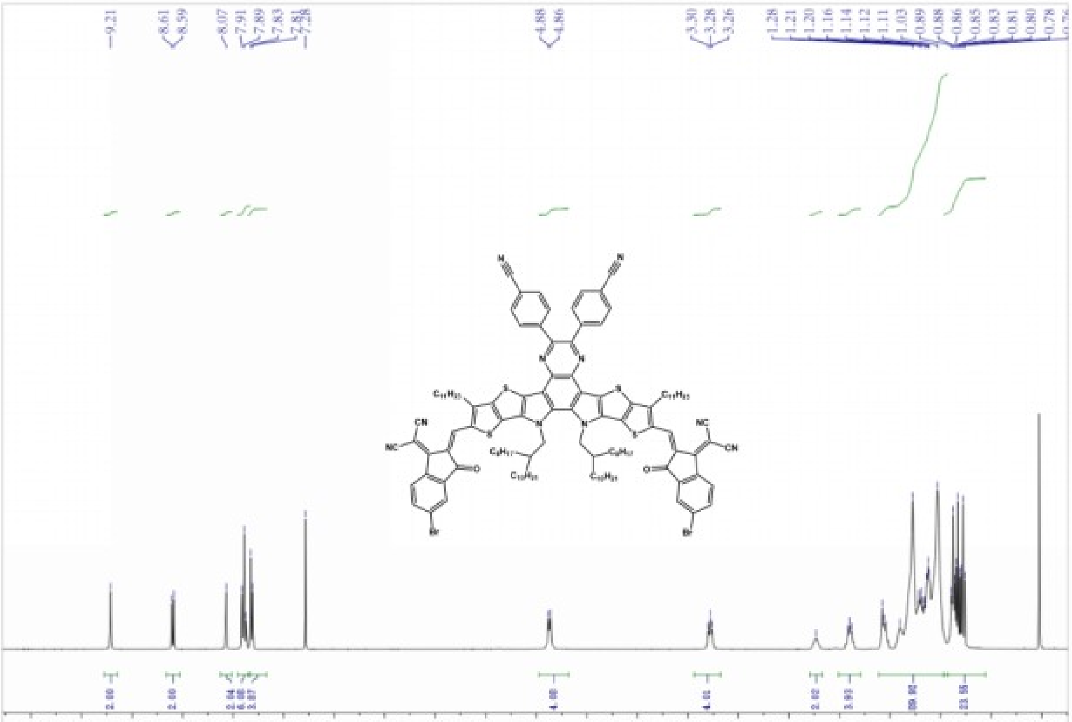

Fig. S2 ^{1}H NMR spectrum of P-BphCN monomer in $CDCl_3$.

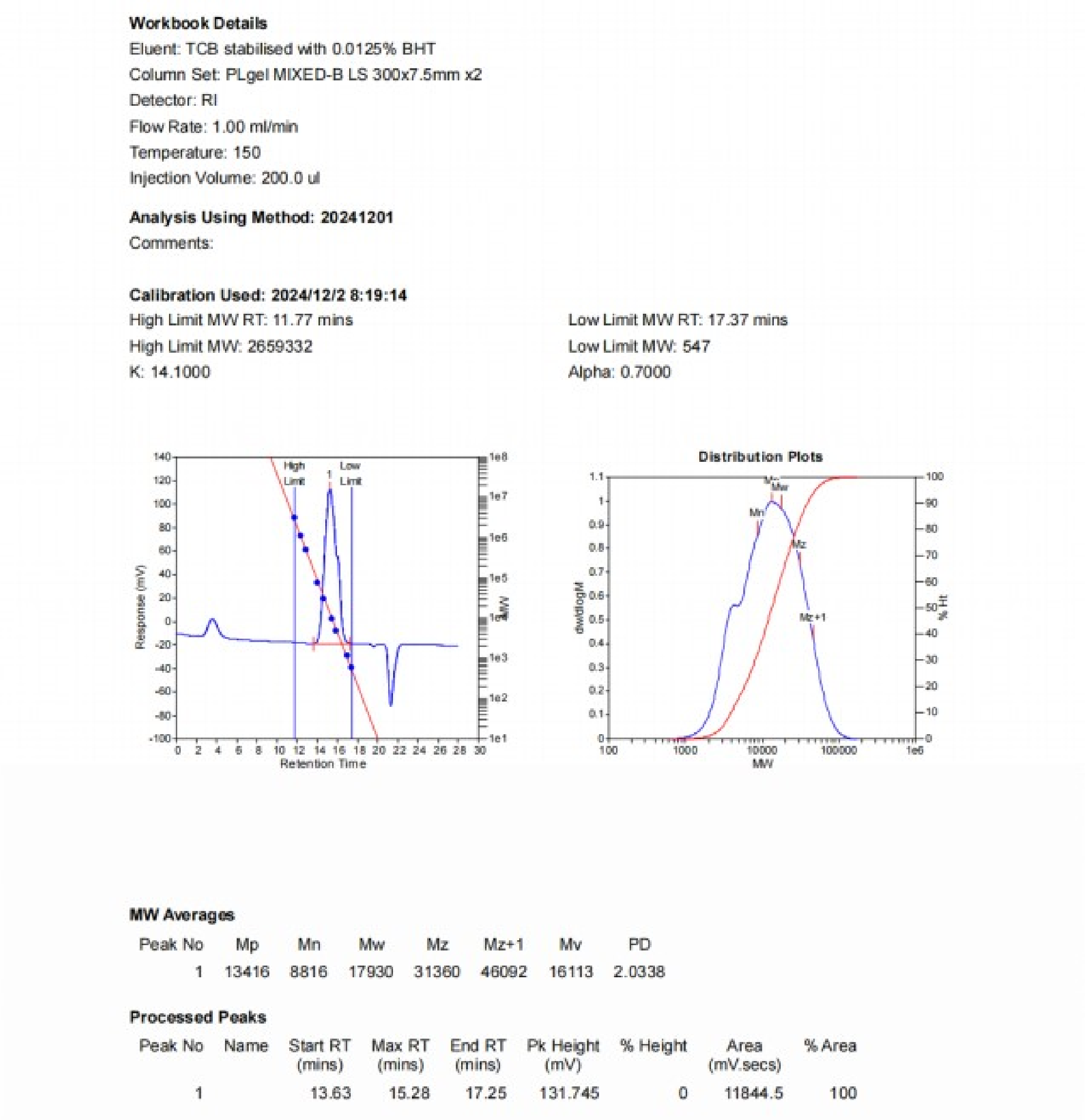

Workbook Details

Eluent: TCB stabilised with 0.0125% BHT

Column Set: PLgel MIXED-B LS 300x7.5mm x2

Detector: RI

Flow Rate: 1.00 ml/min

Temperature: 150

Injection Volume: 200.0 ul

Analysis Using Method: 20241201

Comments:

Calibration Used: 2024/12/2 8:19:14

High Limit MW RT: 11.77 mins

High Limit MW: 2659332

K: 14.1000

Low Limit MW RT: 17.37 mins

Low Limit MW: 547

Alpha: 0.7000

MW Averages

Peak No	Mp	Mn	Mw	Mz	Mz+1	Mv	PD
1	13416	8816	17930	31360	46092	16113	2.0338

Processed Peaks

Peak No	Name	Start RT (mins)	Max RT (mins)	End RT (mins)	Pk Height (mV)	% Height	Area (mV.secs)	% Area
1		13.63	15.28	17.25	131.745	0	11844.5	100

Fig. S3 GPC measurement result of P-phCN.

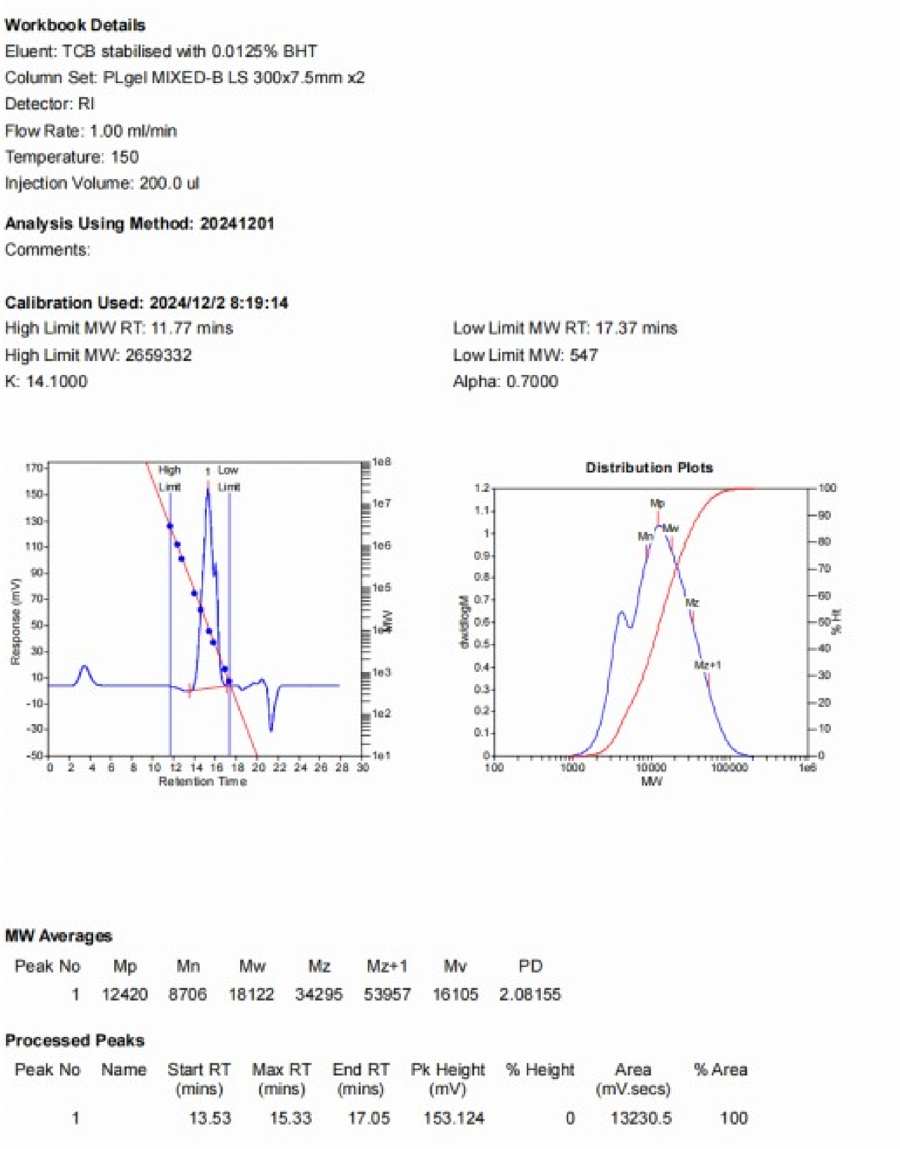

Workbook Details

Eluent: TCB stabilised with 0.0125% BHT
Column Set: PLgel MIXED-B LS 300x7.5mm x2
Detector: RI
Flow Rate: 1.00 ml/min
Temperature: 150
Injection Volume: 200.0 ul

Analysis Using Method: 20241201

Comments:

Calibration Used: 2024/12/2 8:19:14

High Limit MW RT: 11.77 mins	Low Limit MW RT: 17.37 mins
High Limit MW: 2659332	Low Limit MW: 547
K: 14.1000	Alpha: 0.7000

MW Averages

Peak No	Mp	Mn	Mw	Mz	Mz+1	Mv	PD
1	12420	8706	18122	34295	53957	16105	2.08155

Processed Peaks

Peak No	Name	Start RT (mins)	Max RT (mins)	End RT (mins)	Pk Height (mV)	% Height	Area (mV.secs)	% Area
1		13.53	15.33	17.05	153.124	0	13230.5	100

Fig. S4 GPC measurement result of P-BphCN.

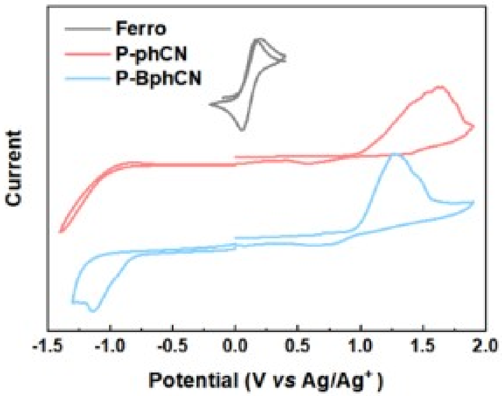

Fig. S5 Cyclic voltammogram for the two polymer acceptors.

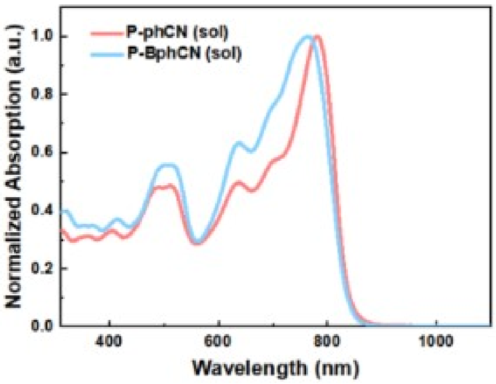

Fig. S6 Normalized UV-vis absorption spectra of solution.

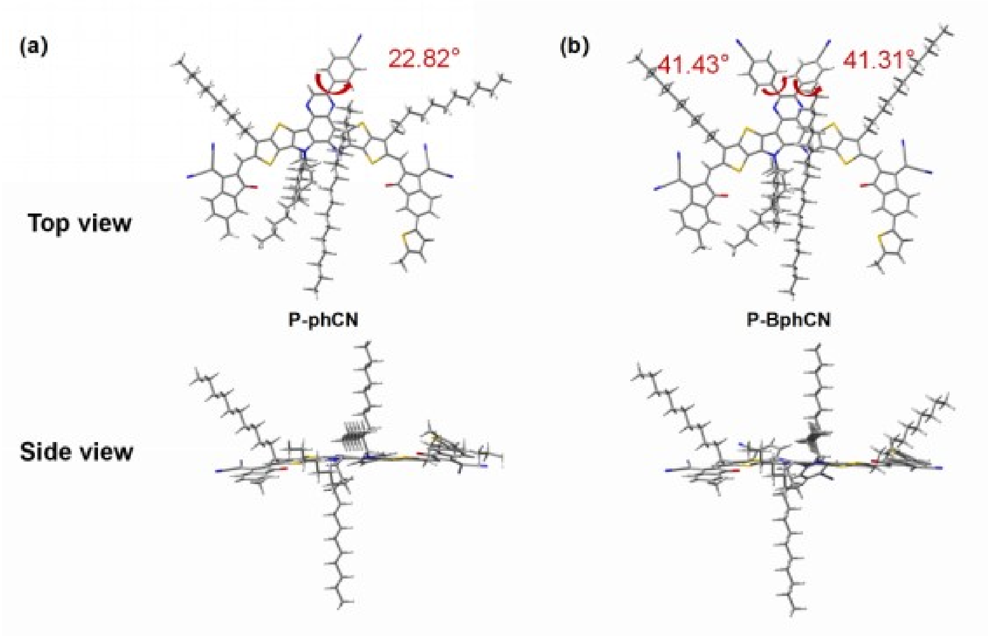

Fig. S7 Optimal conformation simulated by DFT calculations for polymer acceptors (top view and side view).

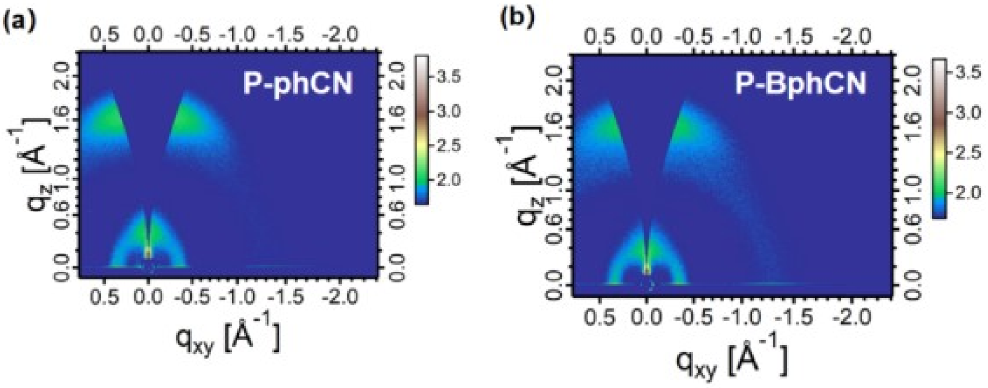

Fig. S8 Two-dimensional GIWAXS patterns of neat films.

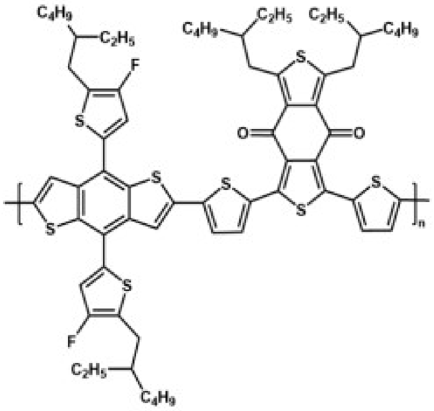

Fig. S9 Chemical structure of PM6.

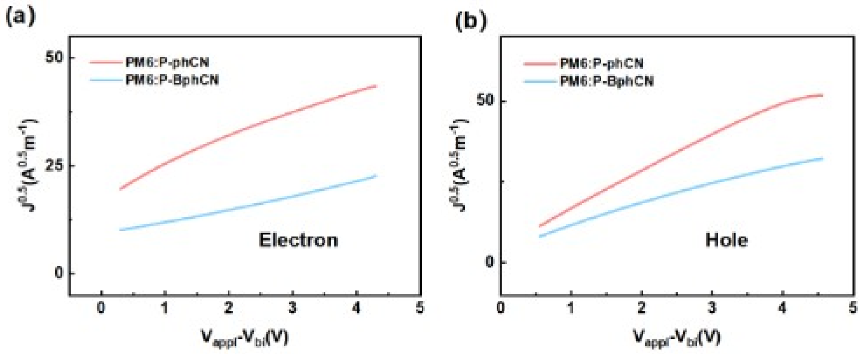

Fig. S10 $J^{0.5}$~V characteristics of the charge carrier mobility measurements of devices.

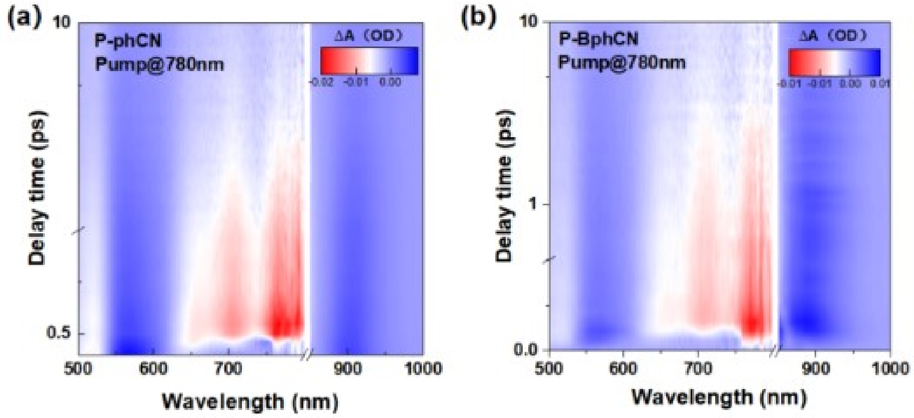

Fig. S11 2D TA spectra of (a)P-phCN pristine film and (b)P-BphCN pristine film.

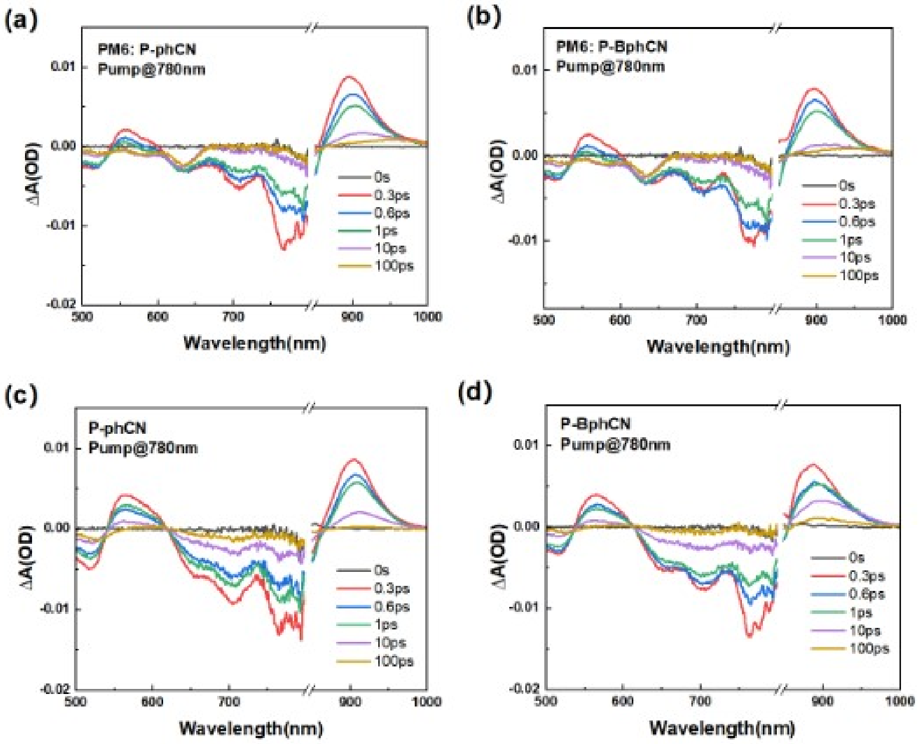

Fig. S12 Corresponding TA spectra recorded at various probe decay times.

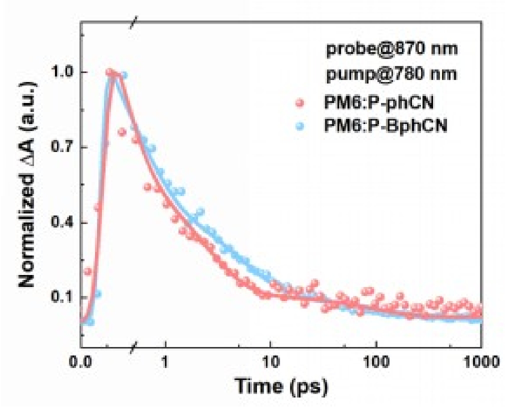

Fig. S13 Transient kinetic traces probing at about 870 nm for the blend films.

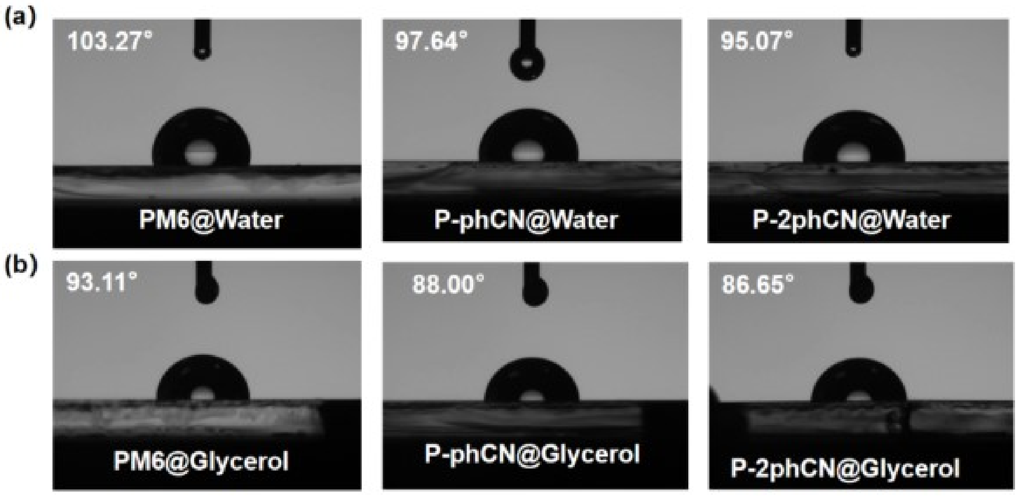

Fig. S14 The images of water and glycerol drops on neat films.

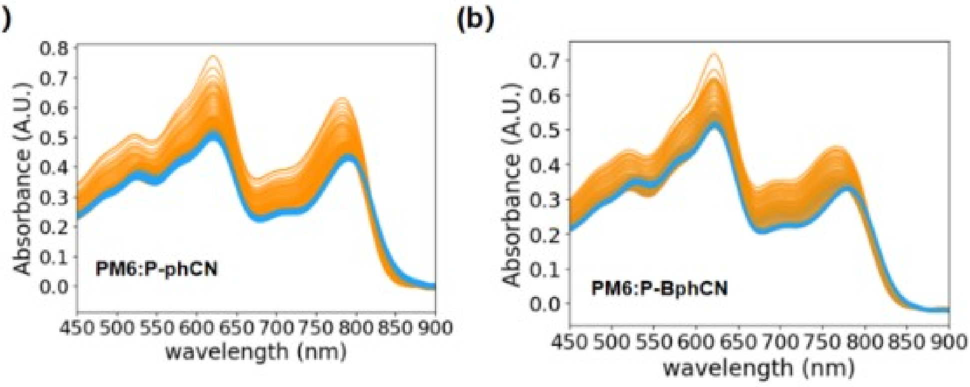

Fig. S15 The time dependent in-situ absorption spectra of the blend films.

3 Supplementary Tables

Table S1. The detailed optoelectronic properties of the two PSMAs.

Acceptor	$\lambda_{\mathrm{max}}^{\mathrm{sol}}$(nm)	$\lambda_{\mathrm{max}}^{\mathrm{film}}$(nm)	$\lambda_{\mathrm{onset}}^{\mathrm{film}}$(nm)	$E_{\mathrm{g}}^{\mathrm{opt}}$	$E_{\mathrm{HOMO}}/E_{\mathrm{LUMO}}$(eV)
P-phCN	781	789	851	1.46	-5.60/-3.60
P-BphCN	765	791	866	1.43	-5.58/-3.75

a) $E_{\mathrm{g}}^{\mathrm{opt}}=1240/\lambda_{\mathrm{onset}}^{\mathrm{film}}$

Table S2. The detailed stacking distance and crystal coherence length (CCL) for different pristine films.

Direction	Film	q[Å^{-1}]	Stacking Distance [Å]	FWHM [Å^{-1}]	CCL [Å]
OOP	P-phCN	1.64	3.83	0.356	17.64
	P-BphCN	1.61	3.90	0.360	17.44

Table S3. Device optimization for PM6:P-phCN.

D: A	Additives	Thermal annealing	V_{OC} (V)	J_{SC} (mA·cm^{-2})	FF (%)	PCE (%)
1:1.1	2.0% CN	100 ℃,10 min	0.944	24.14	74.24	16.92
1:1.2	2.0% CN	100 ℃,10 min	0.946	24.47	73.87	17.10
1:1.3	2.0% CN	100 ℃,10 min	0.940	24.20	71.72	16.77
1:1.4	2.0% CN	100 ℃,10 min	0.946	24.69	70.71	16.52
1:1.2	1.5% CN	100 ℃,10 min	0.945	24.34	72.67	16.73
1:1.2	2.5% CN	100 ℃, 10 min	0.931	25.08	73.02	17.05
1:1.2	2.0% CN	110 ℃, 10 min	0.941	24.17	73.90	16.81

Table S4. Device optimization for PM6:P-BphCN.

D: A	Additives	Thermal annealing	V_{OC} (V)	J_{SC} (mA·cm^{-2})	FF (%)	PCE (%)
1:1.1	2.0% CN	100 °C,10 min	0.896	22.13	70.51	13.98
1:1.2	2.0% CN	100 °C,10 min	0.906	22.65	70.42	14.45
1:1.3	2.0% CN	100 °C,10 min	0.904	22.68	69.98	14.34
1:1.4	2.0% CN	100 °C,10 min	0.905	22.01	70.74	14.08
1:1.2	1.5% CN	100 °C,10 min	0.901	22.56	68.61	13.94
1:1.2	2.5% CN	100 °C, 10 min	0.899	22.88	69.33	14.26
1:1.2	2.0% CN	110 °C, 10 min	0.902	22.53	70.86	14.40

Table S5. Detailed E_{loss} of the devices.

Devices	*Epv g* (eV)	EQE$_{EL}$ (%)	qVSQ OC (eV)	qVrad OC (eV)	E_{loss} (eV)	ΔE_1 (eV)	ΔE_2 (eV)	ΔE_3 (eV)
PM6:P-phCN	1.477	1.63×10^{-2}	1.211	1.184	0.518	0.266	0.027	0.225
PM6: P-BphCN	1.480	3.77×10^{-3}	1.214	1.182	0.562	0.266	0.032	0.264

Table S6. The electron mobility (μ_e) and hole mobility (μ_h) values of the blend films.

Active layer	μ_h (cm^2 V^{-1} s^{-1})	μ_e (cm^2 V^{-1} s^{-1})	μ_h/μ_e
PM6:P-phCN	6.08×10^{-4}	4.16×10^{-4}	1.46
PM6: P-BphCN	3.14×10^{-4}	1.59×10^{-4}	1.97

Table S7. The fitted lifetimes of kinetic trace probed at around 620, 870 and 950 nm decay for the blend films.

Signals	Films	τ_1 (ps)	A1 (%)	τ2 (ps)	A2 (%)	τ3 (ps)	A3 (%)
@870 nm	PM6:P-phCN	0.26	41.0	1.97	44.0	37.4	12.0
	PM6:P-BphCN	0.44	56.8	5.29	34.6	145	7.6
@950 nm	PM6:P-phCN	2.08	38.4	48.9	18.7	1790	19.4
	PM6:P-BphCN	0.19	34.8	12.6	28.1	508	22.4
@620 nm	PM6:P-phCN	4.28	19.7	57.3	37.8	863	19.7
	PM6:P-BphCN	4.15	22.1	80.2	42.5	2600	12.5

Table S8. Charge carrier transport parameters of the optimized devices.

Devices	$J_{ph}^{(a)}$ (mA/cm^2)	$J_{ph}^{(b)}$ (mA/cm^2)	J_{sat} (mA/cm^2)	η_{diss} (%)	η_{coll} (%)
PM6:P-phCN	23.66	24.88	25.04	99.36	94.49
PM6: P-BphCN	20.35	21.92	22.30	98.29	91.26

(a) The photocurrent density obtained under the maximum output power of the device.

(b) The photocurrent density obtained under the short-circuit state of the device.

Table S9. The detailed stacking distance and crystal coherence length (CCL) for different blend films.

Film	Direction	q[Å^{-1}]	Stacking Distance [Å]	FWHM [Å^{-1}]	CCL [Å]
PM6:P-phCN	OOP	1.66	3.78	0.342	18.37

PM6:P-BphCN	OOP	1.63	3.85	0.366	17.15

Table S10. The parameters of surface energies.

Acceptors	$\gamma^{acceptor}$(mN/m^2)	Donor	γ^{donor}(mN/m^2)	χ
P-phCN	13.78	PM6	11.09	0.15
P-BphCN	15.13	PM6	11.09	0.31